Novel chromogenic, guest-sensitive host compounds

Janet Scott,*[a] Masaya Asami[b] and Koichi Tanaka[b]

[a] *Centre for Green Chemistry, P.O. Box 23, Monash University, Victoria 3800, Australia.*
E-mail: janet.scott@sci.monash.edu.au; Fax: 61 3 99054597
[b] *Department of Applied Chemistry, Faculty of Engineering, Ehime University, Matsuyama,*
*Ehime 790-8577, Japan. E-mail: tanaka@en3.ehime-u.ac.jp*

A series of novel chromogenic host compounds based on a diphenylazo core with bulky endgroups and hydrogen bonding capability has been synthesised and shown to exhibit distinct and easily detected colour changes on complexation with guests, allowing for rapid screening of host:guest complex formation.

Introduction

The design of simple, low cost, easily used sensors depends on simple readout mechanisms such as colour changes or chromogenicity. Host:guest complexation events have been touted as suitable sensor systems but, in solid crystalline systems, these often rely on complex readout mechanisms such as mass changes (quartz crystal microbalance readout systems[1,2]) or shifts in absorption or emission maxima (UV, IR, fluorescence spectra[3,4]). The detection of host:guest binding events by colour changes resulting from associated conformational changes and thus shifts in energy of electronic transitions have been reported for a few imidazole compounds.[5] In an earlier communication we reported the synthesis and guest responsive colour changes of a chromogenic host compound, 3-{4-[4-(3-hydroxy-3,3-diphenylprop-1-ynyl)phenylazo]phenyl}-1,1-diphenylprop-2-yn-1-ol **3**.[6]
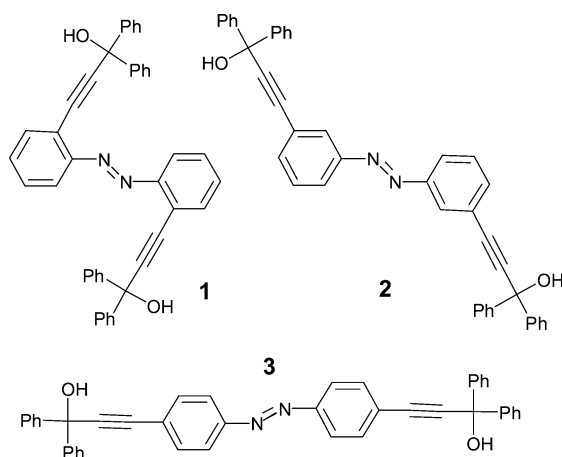
We now report the preparation and complexation behaviour of a further two host compounds in this series, namely, 3-{2-[2-(3-hydroxy-3,3-diphenylprop-1-ynyl)phenylazo]phenyl}-1,1-diphenylprop-2-yn-1-ol **1** and 3-{3-[3-(3-hydroxy-3,3-diphenylprop-1-ynyl)phenylazo]phenyl}-1,1-diphenylprop-2-yn-1-ol **2**.

Results and discussion

Each of the host compounds **1–3** is a bright yellow to yellow/orange crystalline material which, upon guest complexation, exhibits a distinct, easily detected, colour change to bright orange or orange/red. These colour changes may be effected, not only by crystallisation of host:guest complexes from solution, but also by absorption of guest vapours from a saturated atmosphere.[6]

Guest complexation and associated colour changes are listed in Table 1. Host:guest ratios are determined by examination of ^{1}H-NMR data and, where possible, confirmed by single crystal structure analysis.

These azo hosts prove to be very versatile host compounds, including a wide range of guest compounds with suitable H-bond acceptor groups. To attempt to understand the source of the colour changes and allow description of host:host and host:guest interactions, the crystal structures of hosts **1** and **3** and a series of inclusion compounds with dimethylsulfoxide (DMSO) and dimethylformamide (DMF) guests were elucidated. Crystal and refinement data are presented in Table 2 and molecular diagrams in Fig. 1.

All host:guest inclusion compounds exhibit host···guest OH···O hydrogen bonding, while guest free crystals of hosts **1** and **3** exhibit host···host OH···N hydrogen bonds (guest free crystals of host **2**, suitable for crystallographic structure determination, were not obtained). Hydrogen bonds and hydrogen bond geometries are detailed in Table 3. The different hydrogen bond regimes are reflected in distinctly different packing modes, with both guest-free host crystals exhibiting hydrogen bonded tapes formed by 2 pairs of donor and acceptor hydrogen bonds per host molecule as depicted in Fig. 2. These tapes or ribbons interconnect *via* CH···π interactions forming, in the case of the *o*-host **1**, a series of flat sheets and, in the case of *p*-host **3**, a network. In spite of the similarity of the included guests the complexes are all distinctly different. In all host:guest complexes, except that of **2**·DMSO, guests act as single H-bond acceptors and form discrete host·2guest H-bonded units. These units interact *via* extensive edge to face CH···π interactions and, to a lesser extent, ππ stacking interactions. **2**·DMSO, on the other hand, has two acceptor H-bond interactions per guest O atom (necessitating guest disorder over two positions), yielding zig-zag ribbons of host and guest. These ribbons interact *via* CH···π and ππ stacking interactions as illustrated in Fig. 3.

A comparison of the host packing modes reveals little similarity even in complexes of the same host with guests of similar size and H-bond acceptor capacity. Thus, while **1**·2DMSO, **2**·2DMF, and **3**·2DMSO form channels propagating parallel

Table 1 Host:guest ratio and colour of inclusion complexes of **1–3**

Guest	**1**		**2**		**3**	
	h:g	colour	h:g	colour	h:g	colour
THF	—[a]		1:2	orange	—	
Dioxane	—		1:2	orange	—	
CH$_3$CN	—		1:1	orange	—	
Cyclopentanone	—		1:2	orange	—	
γ-Butyrolactone	—		1:2	orange	1:2	orange
DMF	1:2	red	1:2	orange	1:2	red
DMSO	1:2	red	1:1	orange	1:2	orange
Pyridine	1:2	orange	1:2	orange	1:3	orange
Me$_2$N–CH$_2$–NMe$_2$					1:2	red

[a] No complexation.

to *a* and **2**·DMSO forms channels propagating parallel to *c* into which guest molecules pack, **3**·2DMF exhibits 'crossed' hosts and guests accommodated in cavities and **1**·2DMF forms discrete G–H–G units which exhibit some short C(Ar)–H···O interactions, illustrated in Fig. 4.

The different packing modes result in distinctly different environments about the N=N bond for host alone *vs* host:-guest inclusion complexes. In guest free **1** and **3** the N=N group is a double H-bond acceptor and the adjacent aromatic rings are π stacked while in all inclusion complexes the N=N bond is surrounded by non-polar guest methyl groups and/or aromatic rings, Fig. 5.

A preliminary investigation led us to the conclusion that the distinct colour changes on guest complexation were, in part, due to differences in the host conformation (specifically co-planarity of one of the terminal aromatic rings with the azobenzene core) and hence in the degree of conjugation through the entire host.[6]

Examination of this larger dataset reveals that, for most of the inclusion complexes studied, the dihedral angles of the terminal phenyl rings are not co-planar with the aromatic rings of the backbone (Table 4). Contrarily however, the complex **2**·2DMF and host **1** alone have terminal phenyl rings exhibiting similar dihedral angles, yet the crystals of these compounds are orange and yellow in colour respectively. Clearly our earlier suggestion is an inadequate description of the source of the colour changes noted in complexed *vs.* uncomplexed

host and closer examination of the solid-state structures is warranted.

The electronic transitions of coloured *trans*-azobenzene compounds have been widely studied and the lowest energy absorption is ascribed to an n → π* transition[8] which may be shifted to longer wavelength upon hydrogen bonding and loss of planarity.[9] Protonation to yield the azonium cation also results in significant shifts to longer wavelength, although steric factors are also important.[10] The n → π* transition energies are determined "primarily by the local symmetry of the azo group and not by the molecular geometry"[11] and Robin and Simpson suggest that the formally forbidden n → π* transition gains intensity by mixing with the strong, low frequency azo-dye 'colour' band.[12] An increase in π electron conjugation is reflected in N–C(aromatic) bond contraction and N=N bond expansion or a decrease in double bond character of the azo bond.[13]

The crystal structures of the complexes allow comparison of molecular geometries, as they occur in the solid-state. Examination of the geometrical parameters of the azobenzene core, specifically those defining C–N=N–C geometry and aromatic *vs* C–N=N–C twist, reveal minor and variable changes in *d* N–C(Ar) and ∠ C–N=N, but distinct and correlated changes in *d* N=N and the torsion angle N=N–C(Ar)–C(Ar) (which defines the aromatic *vs* C–N=N–C twist), as illustrated in Fig. 6. For the solid-state structures of the *ortho* host **1** and its host:guest complexes, as the twist angle increases the N=N bond length expands and a similar trend is noted for **2** (albeit with only two structural examples). While the correlation of increasing N=N bond length with increasing twist angle is less clear for **3**, it is notable that the host alone structure again displays both the greatest twist angle and longest N=N bond length. An increase in N=N bond length implies greater conjugation with the aromatic π system and, while it might seem counterintuitive that this should be associated with an *increase* in twist angle, this has been considered by Yu *et al.* who find that planarity does not necessarily confer greater π resonance stabilisation.[14] In addition the host azo group in both of the 'host alone' crystal structures acts as a double hydrogen bond acceptor. This interaction may be considered the first step along the continuum to azonium cation formation and, as such, would be expected to yield a shift to longer λ in the absorption spectrum.[10] This is not noted in the solid-state absorption spectra of crystalline **2** and **2**·2DMF or in the previously recorded spectrum of complexed and uncomplexed

Table 2 Crystal and refinement data for crystalline complexes of **1**, **2** and **3** (data for **3** and **3**·2DMF have been reported previously[6])

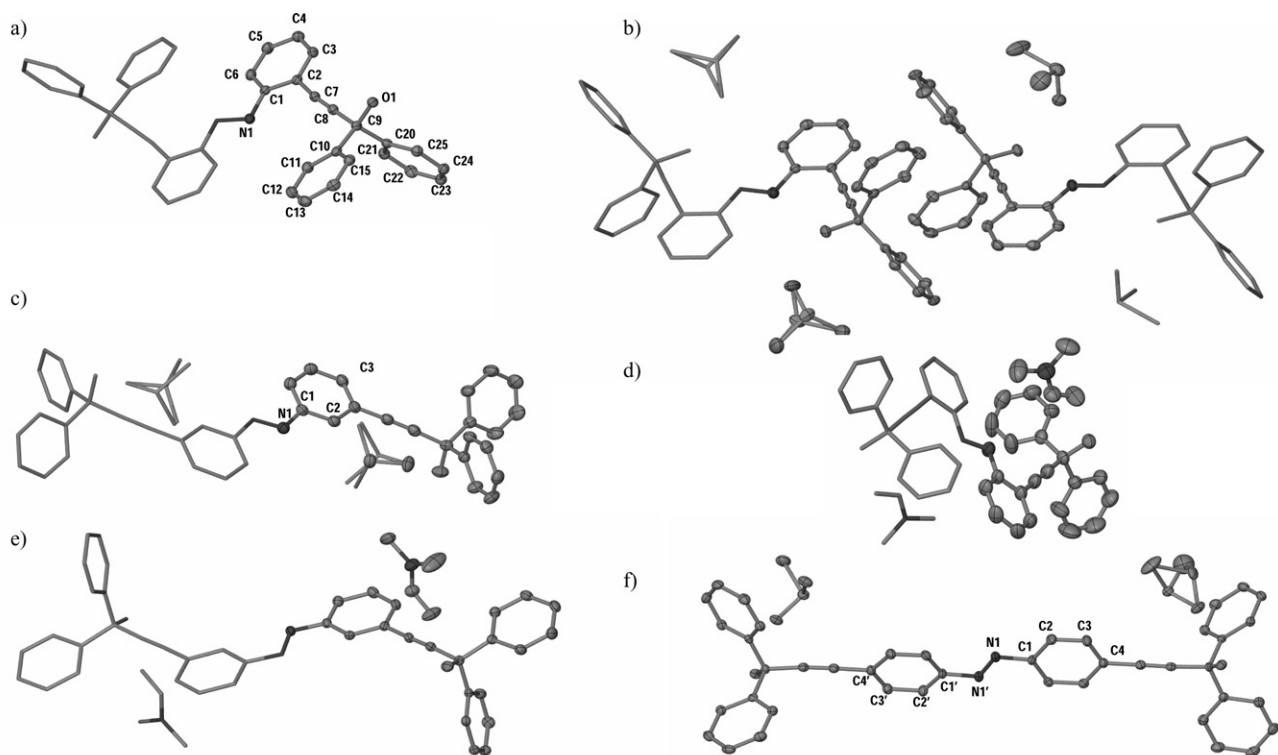|	**1**	**1**·2DMSO	**1**·2DMF	**2**·DMSO	**2**·2DMF	**3**·2DMSO
Empirical formula	C$_{42}$H$_{30}$N$_2$O$_2$	C$_{46}$H$_{42}$N$_2$O$_4$S$_2$	C$_{48}$H$_{44}$N$_4$O$_4$	C$_{44}$H$_{36}$N$_2$O$_3$S	C$_{48}$H$_{44}$N$_4$O$_4$	C$_{46}$H$_{42}$N$_2$O$_4$S$_2$
*M*r	594.68	750.94	740.88	672.81	740.88	750.94
Crystal system	triclinic	triclinic	triclinic	monoclinic	monoclinic	monoclinic
Space group	P$\bar{1}$	P$\bar{1}$	P$\bar{1}$	C2/c	P2$_1$/c	P2$_1$/c
a/Å	5.8554(2)	11.7388(3)	9.7114(2)	29.7426(2)	8.6442(1)	11.8006(2)
b/Å	9.3045(5)	12.0389(2)	10.4231(2)	12.4739(2)	11.6634(2)	22.0051(4)
c/Å	14.6994(5)	16.7993(3)	11.8636(3)	9.5222(4)	20.1599(4)	15.1395(3)
α/°	71.827(3)	76.252(1)	70.951(1)	90	90	90
β/°	89.422(3)	72.534(1)	70.758(1)	92.875(1)	101.248(1)	91.658(1)
γ/°	78.702(2)	61.240(1)	70.161(1)	90	90	90
V/Å^3	745.04(5)	1972.92(7)	1034.91(4)	3528.35(16)	1993.50(6)	3929.68(12)
Z	1	2	1	4	2	4
D$_c$/g cm^{-3}	1.325	1.264	1.189	1.267	1.234	1.269
μ/mm^{-1}	0.081	0.181	0.076	0.136	0.079	0.182
Refl. unique	2518	9553	4924	4379	4909	9616
Refl. *I* > 2σ(*I*)	2079	4543	2365	2974	2887	5466
R$_1$/*wR*$_2$ [*I* > 2σ(*I*)]	0.0412/0.0995	0.0524/0.1046	0.0524/0.1320	0.0531/0.1456	0.0459/0.0971	0.0533/0.1128
R$_1$/*wR*$_2$ [all data]	0.0529/0.1075	0.1481/0.1287	0.1290/0.1559	0.0856/0.1628	0.1013/0.1120	0.1119/0.1264
GoF on *F*^{2}	1.043	0.893	0.966	1.045	0.941	1.066
Paramaters/restraints	209/0	530/6	259/0	240/0	259/0	504/0

Fig. 1 Molecular diagrams of a) **1**, b) **1**·2DMSO, c) **2**·DMSO, d) **1**·2DMF, e) **2**·2DMF and f) **3**·2DMSO. Asymmetric unit atoms are indicated as ellipsoids at the 50% probability level. Molecular numbering is indicated in detail for hosts alone; the same numbering scheme is followed in each case.

Table 3 Hydrogen bond geometrical parameters

		d(D–H)/Å	d(H···A)/Å	∠(DHA)/°	d(D···A)/Å
1	O1–H1O···N1[a]	1.13	1.79	170	2.920(2)
1·2DMSO	O 1–H1O···O1G	0.86(3)	1.89(3)	161(3)	2.718(2)
	O1'–H1O'···O2G[b]	0.86(3)	1.90(3)	166(3)	2.738(2)
1·2DMF	O1–H1O	0.98(2)	1.69(2)	175(2)	2.670(2)
2·DMSO	O1·H1O···O2	0.89(2)	1.85(2)	161(2)	2.707(2)
2·2DMF	O1·H1O···O1G[c]	0.96(2)	1.79(2)	165(2)	2.734(2)
3·2DMSO	O 1–H1O···O2G[d]	0.88(2)	1.88(3)	169(2)	2.755(2)
	O1'–H1O'···O1G	0.89(2)	1.87(3)	172(2)	2.755(2)
3·2DMF	O1–H1O···O1A	0.90(3)	1.86(3)	170(2)	2.749(2)
	O1'–H1'O···O1B[e]	0.91(3)	1.79(3)	179(2)	2.700(2)
3	O1–H1O···N1[f]	0.94	2.11	162	3.019(2)

[a] $(x-1, y, z)$. [b] $(x+1, y-1, z)$. [c] $(-x, y-\frac{1}{2}, -z+\frac{1}{2})$. [d] $(x, \frac{1}{2}-y, z-\frac{1}{2})$. [e] $(x-1, y+, z)$. [f] $(-x+1, -y+1, -z)$.
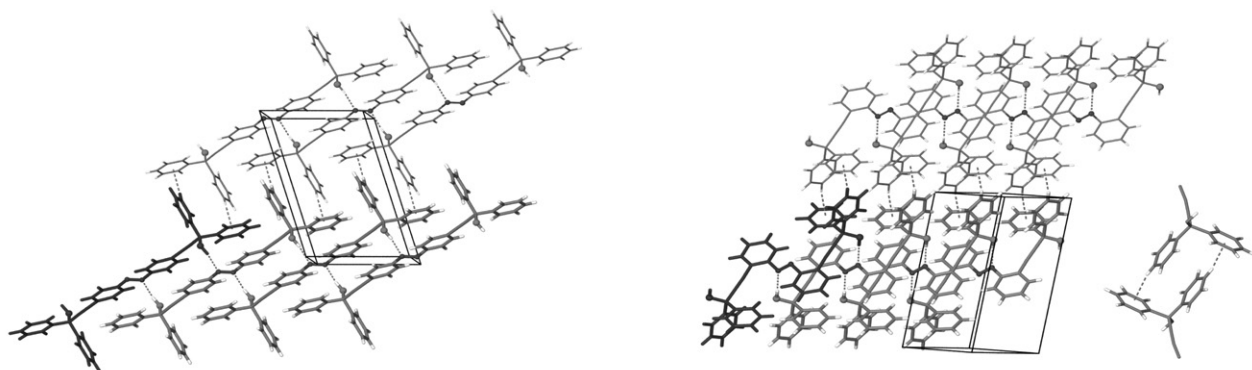

Fig. 2 Host packing: a) *p*-host **1** and b) *o*-host **3**. For clarity O and N atoms are depicted as filled spheres, H-bonds and CH···π interactions as dotted lines and a single host molecule as dark lines. In each case OH···N H-bonds 'stitch' the hosts together forming ribbons which in turn interact *via* CH···π interactions forming the 'phenyl embrace' type motif described by Scudder and Dance.[7] The phenyl embrace geometry for **3** is depicted as an insert, while that noted in **1** has been described previously.
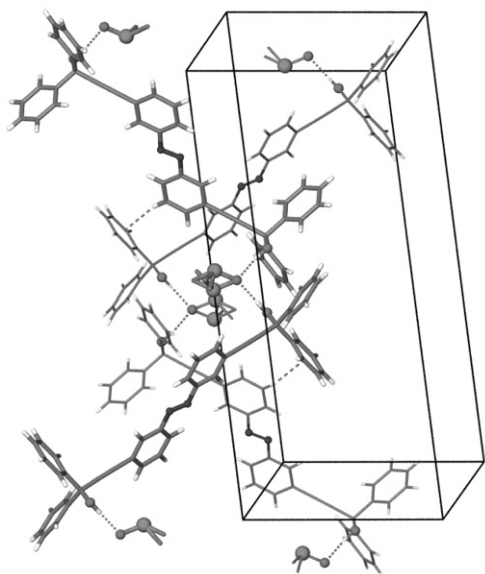
Fig. 3 Double H-bond acceptor DMSO guests form zig-zag tapes with host **2**. These tapes interact *via* CH···π interactions. Oxygen, sulfur and nitrogen atoms are depicted as spheres and H-bonds as dotted lines. Two tapes are drawn with differing thickness bonds.

host **3**.[6] Thus, while it certain that this interaction is important in changing the energy of electronic transitions responsible for colour changes in these azobenzene derived hosts, the expected shift to longer λ does not occur.

Since colour changes are noted in solution as well as in the solid state, we examined the UV-vis absorption spectra of these hosts dissolved in liquid guests. While increased solvent polarity has been described as important in effecting bathochromic shifts in azoaromatic compounds[15] we find that the concentration of the dissolved host compound is also a contributing factor. Thus for host **3** in DMF an increase in concentration results in a shift in absorption maximum as illustrated in Fig. 7, implying that host/host or host/guest/host interactions between molecules in solution are also important in the development of the observed colour changes.

Thus, we postulate that the colour changes noted on guest inclusion are due to the changed energy of electronic transitions of the azobenzene core of the host moleulces.
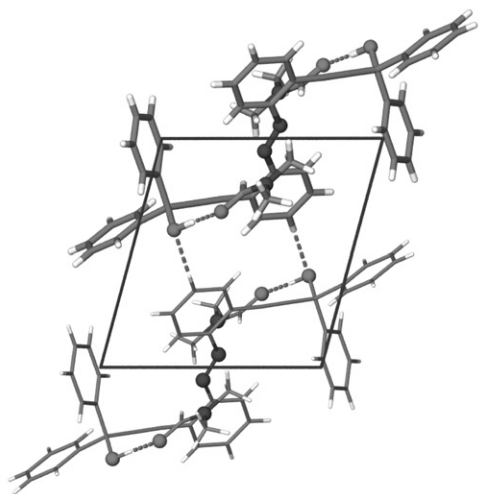

Fig. 4 **1**·DMF forms discrete hydrogen bonded host·2 guest units which in turn interact *via* a short C4–H4···O1 $(1 - x, 1 - y, 1 - z)$ contact: d C4···O1 3.386 Å; d H4···O1 2.47 Å; $\angle$ C4–H4···O1 167°. Interdigitation of phenyl rings and DMF methyl groups serves to further stabilise the structure.
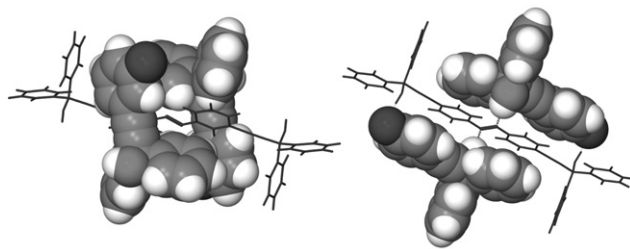

Fig. 5 N=N environments, illustrated here for **2**·DMSO (left) and guest free **3** (right). In all host:guest complexes the N=N bond is surrounded by non-polar groups, including backbone and terminal aromatic rings or guest methyl groups. Where packing allows, the backbone aromatic rings adjacent to the azo bond participate in CH···π π interactions (complexes) and π stacking interactions (host alone).

Destruction of the host to host OH···N hydrogen bonding and changes in the degree of conjugation, which are reflected in the greater twist angle of the azo linkage and aromatic rings, result in an increase in the wavelength of the visible region absorption maximum, making the detection of guest inclusion as simple as a colour matching exercise.

Experimental

Synthesis

3-{2-[2-(3-Hydroxy-3,3-diphenylprop-1-ynyl)phenylazo]phenyl}-1,1-diphenylprop-2-yn-1-ol [1]. Preparation of host **1**: 2,2′-dibromoazobenzene[16] (2.0 g, 5.9 mmol), 1,1-diphenylprop-2-yn-1-ol (2.5 g, 11.8 mmol), PdCl$_2$(PPh$_3$)$_2$ (0.05 g), PPh$_3$ (0.26 g), CuI (0.05 g) and Et$_3$N (150 ml) were mixed and heated under reflux for 6 h. After filtration of Et$_3$N·HBr, the Et$_3$N solution was evaporated to leave crude **1**. Recrystallization of this from toluene gave pure **1** as yellow prisms (0.55 g, 15% yield). Mp 168–171 °C; IR (Nujol) 3396 cm^{-1}; UV (CHCl$_3$) λ_{max}/nm (ε) 241 (45 600), 259 (42 200), 340 (17 200); δ_H (300 MHz, CDCl$_3$) 7.66–7.73 (m, 12 H), 7.26–7.46 (m, 16 H), 2.98 (s, 2 H). Anal. Calc. For C$_{42}$H$_{30}$N$_2$O$_2$: C, 84.82; H, 5.08; N, 4.71. Found: C, 84.80; H, 5.14; N, 4.75%.

3-{3-[3-(3-Hydroxy-3,3-diphenylprop-1-ynyl)phenylazo]phenyl}-1,1-diphenylprop-2-yn-1-ol [2]. Preparation of host **2**: 3,3′-dibromoazobenzene[16] (2.0 g, 5.9 mmol), 1,1-diphenylprop-2-yn-1-ol (2.5 g, 11.8 mmol), PdCl$_2$(PPh$_3$)$_2$ (0.05 g), PPh$_3$ (0.26 g), CuI (0.05 g) and Et$_3$N (150 ml) were mixed and heated under reflux for 6 h. After filtration of Et$_3$N·HBr, the Et$_3$N solution was evaporated to leave crude **2**. Recrystallization of this from toluene gave pure **2** as yellow prisms (2.05 g, 58% yield). Mp 153–156 °C; IR (Nujol) 3422 cm^{-1}; UV (CHCl$_3$) λ_{max}/nm (ε) 249 (57 800), 318 (26 800); δ_H (300

Table 4 Dihedral angles: terminal phenyl rings to backbone[a]

	B–A/°	C–A/°
1	85.71(4)	12.25(8)
1·2DMSO	73.84(6)	67.92(7)
	73.52(6)	68.30(7)
1·2DMF	57.20(6)	55.69(8)
2·DMSO	89.39(6)	42.42(7)
2·2DMF	86.42(4)	15.18(7)
3·2DMSO	86.65(6)	39.32(7)
	88.68(6)	10.36(10)
3·2DMF	72.87(5)	65.88(7)
	76.22(5)	59.48(7)
3	89.03(5)	2.73(6)

[a] A is the azobenzene or 'backbone' aromatic ring while B and C represent the two terminal phenyl substituents.
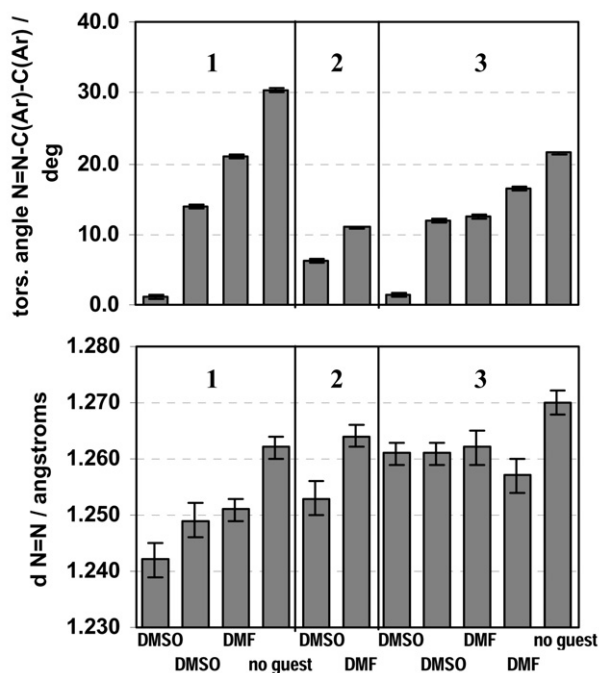
Fig. 6 Torsion angle N=N–C(Ar)–C(Ar), top and *d* N=N, bottom. For both hosts **1** and **3** alone the N=N distance reaches a maximum and this is matched by a large out of plane twist of the backbone aromatic rings relative to the plane C–N=N–C about the azo linkage.

MHz, CDCl$_3$) 7.29–8.07 (m, 28 H), 2.88 (s, 2 H). Anal. Calc. For C$_{42}$H$_{30}$N$_2$O$_2$: C, 84.82; H, 5.08; N, 4.71. Found: C, 84.66; H, 5.29; N, 4.37%.

Crystallography

Crystals suitable for single crystal X-ray diffraction experiments were grown by slow evaporation of solutions of the host in dichloromethane and the chosen guest species. In some cases a second solvent such as toluene was added. Data were collected on an Enraf-Nonius Kappa CCD diffractometer at 123 K (except for complex **1**·2DMF, which due to a low *T* phase change was collected at 294 K) using graphite monochromated Mo-Kα radiation ($\lambda = 0.71073$ Å, 1° φ and ω scans). Structures were solved by direct methods using the program SHELXS-97[17] and refined by full matrix least squares refinement on F^2 using the programs SHELXL-97[18] and X-Seed.[19] Non-hydrogen atoms of the hosts were refined anisotropically and hydrogen atoms inserted in geometrically determined positions with temperature factors fixed at 1.2 times (1.5 for methyl hydrogens) that of the parent atom.
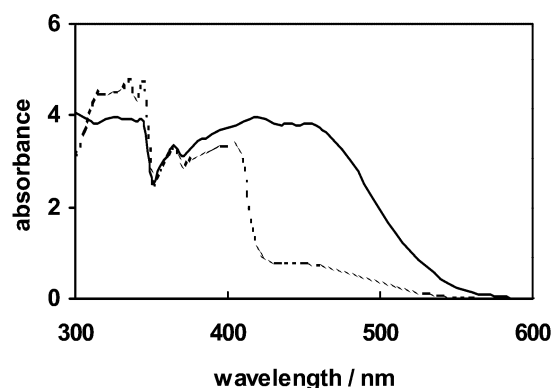

Fig. 7 Solution phase UV-vis absorption spectra for host **3** in DMF; solid line $c = 2.13 \times 10^{-3}$ M; dotted line $c = 1.68 \times 10^{-4}$ M. The shift in absorption maximum on increase in concentration is marked.

DMSO or DMF guests were refined in similar fashion except where guests were disordered.

Host **1** alone has one $\frac{1}{2}$ host in the asymmetric unit, the remaining $\frac{1}{2}$ host being generated by a centre of symmetry. Compound **1**·2DMSO has two $\frac{1}{2}$ host and 2 guest DMSO molecules in the asymmetric unit. One DMSO guest molecule was modelled with the S atom disordered over two positions (s.o.f. = 85% and 15% for major and minor components) and methyl group hydrogen atom positions were modelled based on the major component only. Compound **1**·2DMF has one $\frac{1}{2}$ host and 1 guest DMF molecule in the asymmetric unit. Compound **2**·DMSO has one $\frac{1}{2}$ host and one $\frac{1}{2}$ disordered DMSO guest molecule in the asymmetric unit. The guest O atom is located on special position $\frac{1}{2}$, *y*, $\frac{1}{4}$ and the S and C atoms disordered over two symmetry related positions. This disorder is associated with hydrogen bonding to alternate host molecules. No hydrogen atoms were included in the disordered guest model. Compound **2**·2DMF has one $\frac{1}{2}$ host and one guest DMF molecule in the asymmetric unit. Compound **3**·2DMSO is unique amongst the crystal structures of these hosts as there is a whole host per asymmetric unit and the host backbone is thus not symmetrical about a centre of symmetry, as is true for all other structures solved. There are 1 host and 2 guest molecules in the asymmetric unit and one guest DMSO molecule is disordered. While difference electron density maps reveal a number of peaks in the vicinity of the guest the model imposed was one of a disordered S atom (s.o.f. = 90% and 10% for major and minor components). The structure of **3**·2DMF has been reported[6] and is included for comparison only. It exhibits two $\frac{1}{2}$ hosts with associated guest DMF molecules in the asymmetric unit.

CCDC reference numbers 195725 and 196890–196894. See http://www.rsc.org/suppdata/nj/b2/b204221e/ for crystallographic data in CIF or other electronic format.

References

1 K. Matsuura, K. Ariga, K. Endo, Y. Aoyama and Y. Okahata, *Chem. Eur. J.*, 2000, **6**, 1750 and references therein.
2 Z. Cao, K. Murayama and K. Aoki, *Anal. Chim. Acta*, 2001, **448**, 47.
3 T. H. Brehmer, P. P. Korkas and E. Weber, *Sens. Actuators B*, 1997, **44**, 595.
4 D. Xu, K. T. Khin, W. E. van der Veer, J. W. Ziller and B. Hong, *Chem. Eur. J.*, 2001, **7**, 2425.
5 Y. Inoue and Y. Sakaino, *Bull. Chem. Soc. Jpn.*, 1986, **59**, 3295; Y. Sakaino, T. Takizawa, Y. Inoue and H. Kakisawa, *J. Chem. Soc., Perkin Trans. 2*, 1986, 1623; Y. Sakaino and R. Fujii, *J. Chem. Soc., Perkin Trans. 1*, 1990, 2852; M. Kaftory, H. Taycher and M. Botoshansky, *J. Chem. Soc., Perkin Trans. 2*, 1998, 407; K. Yoshida, Y. Ooyama, S. Tanikawa and S. Watanabe, *Chem. Lett.*, 2000, 714.
6 K. Tanaka, M. Asami and J. L. Scott, *New J. Chem.*, 2002, 378.
7 M. Scudder and I. Dance, *J. Chem. Soc., Dalton Trans.*, 1998, 155.
8 H. H. Jaffe, S.-J. Yeh and R. W. Gardner, *J. Mol. Spectrosc.*, 1958, **2**, 120.
9 S. Millefiori, A. Millefiori and F. Guerrera, *Spectrochim. Acta*, 1980, 835.
10 J. Griffiths, B. Roozpeikar and J. Thomasson, *J. Chem. Res. (S)*, 1981, 302.
11 H. Rau, *Angew. Chem., Int. Ed. Engl.*, 1973, **12**, 224.
12 M. R. Robin and W. T. Simpson, *J. Chem. Phys.*, 1962, **36**, 580.
13 N. Biswas and S. Umapathy, *J. Phys. Chem. A*, 2000, **104**, 2734.
14 Z.-H. Yu, L.-T. Li, W. Fu and L.-P. Li, *J. Phys. Chem. A*, 1998, **102**, 2016.
15 A. Airinei, E. Rusu and D. Dorohoi, *Spectrosc. Lett.*, 2001, **34**, 65.
16 O. H. Wheeler and D. Gonzalez, *Tetrahedron*, 1964, **20**, 189.
17 G. M. Sheldrick, SHELXS-97, University of Gottingen, 1997.
18 G. M. Sheldrick, SHELXL-97, University of Gottingen, 1997.
19 L. J. Barbour, X-Seed - a graphical interface to the SHELX program suite, University of Missouri, 1999.